

Hydrodynamic cavitation kills prostate cells and ablates benign prostatic hyperplasia tissue

Zeynep Itah¹, Ozlem Oral^{1,2}, Osman Yavuz Perk³, Muhsincan Sesen³, Ebru Demir³, Secil Erbil¹, A Isin Dogan-Ekici⁴, Sinan Ekici⁵, Ali Kosar³ and Devrim Gozuacik¹

¹Biological Sciences and Bioengineering Program, Faculty of Engineering and Natural Sciences, Sabanci University, Orhanli-Tuzla, 34956 Istanbul, Turkey; ²Nanotechnology Research and Application Center, Faculty of Engineering and Natural Sciences, Sabanci University, Orhanli-Tuzla, 34956 Istanbul, Turkey; ³Mechatronics Engineering Program, Faculty of Engineering and Natural Sciences, Sabanci University, Orhanli-Tuzla, 34956 Istanbul, Turkey; ⁴Department of Pathology, Yeditepe University School of Medicine, Atasehir, 34755 Istanbul, Turkey; ⁵Department of Urology, Maltepe University School of Medicine, Maltepe, 34843 Istanbul, Turkey
Corresponding author: Devrim Gozuacik. Email: dgozuacik@sabanciuniv.edu

The first two authors contributed equally.

Abstract

Hydrodynamic cavitation is a physical phenomenon characterized by vaporization and bubble formation in liquids under low local pressures, and their implosion following their release to a higher pressure environment. Collapse of the bubbles releases high energy and may cause damage to exposed surfaces. We recently designed a set-up to exploit the destructive nature of hydrodynamic cavitation for biomedical purposes. We have previously shown that hydrodynamic cavitation could kill leukemia cells and erode kidney stones. In this study, we analyzed the effects of cavitation on prostate cells and benign prostatic hyperplasia (BPH) tissue. We showed that hydrodynamic cavitation could kill prostate cells in a pressure- and time-dependent manner. Cavitation did not lead to programmed cell death, i.e. classical apoptosis or autophagy activation. Following the application of cavitation, we observed no prominent DNA damage and cells did not arrest in the cell cycle. Hence, we concluded that cavitation forces directly damaged the cells, leading to their pulverization. Upon application to BPH tissues from patients, cavitation could lead to a significant level of tissue destruction. Therefore similar to ultrasonic cavitation, we propose that hydrodynamic cavitation has the potential to be exploited and developed as an approach for the ablation of aberrant pathological tissues, including BPH.

Keywords: Hydrodynamic cavitation, cell death, autophagy, prostate cells, benign prostatic hyperplasia, tissue ablation

Experimental Biology and Medicine 2013; 238: 1242–1250. DOI: 10.1177/1535370213503273

Introduction

Cavitation is a physical phenomenon defined by the generation of microscopic vapor bubbles in liquid media, followed by their growth and violent collapse or implosion.^{1,2} Cavitation leads to the release of a strong bursts of energy and results in a great rise in temperature (to about 2000–5000 K) and pressure (to about 20–3000 bars) in the immediate vicinity of the bubbles.³ In industry, cavitation was shown to be one of the causes of abrasion of engine or machine parts such as the pistons of car engines or ship propellers. As such, it was long studied as an undesired and deleterious event, hence researchers put a significant effort to discover ways to minimize its generation and its effects in industry.

Destructive nature of cavitation was exploited for biomedical purposes. The majority of the papers that were published in this field concentrated on the biomedical effects of heat and cavitation produced by ultrasonic waves. The effects of

ultrasound on tissues and cells depend on several parameters including ultrasound intensity, frequency and focalization. Short, high-intensity ultrasound pulses produced in a repetitive manner were shown to cause damage in targeted tissues, and the technique was called “histotripsy”. While high-intensity focused ultrasound (HIFU) mainly resulted in thermal effects, histotripsy-related effects on tissues were mainly attributed to cavitation. HIFU and histotripsy were successfully used as tools for the ablation of benign or malignant masses localized to various tissues including prostate,^{4–11} breast,^{12,13} liver,¹⁴ kidney,¹⁵ pancreas¹⁶ and uterus.^{17,18} Additionally, ultrasonic cavitation was effective in destroying kidney stones.^{19,20}

Ultrasound treatment became a pioneering and popular clinical tool due to the fact that it is a non-invasive and extracorporeal treatment methodology. Non-focused ultrasound methods may result in hyperthermia, i.e. tissue temperatures

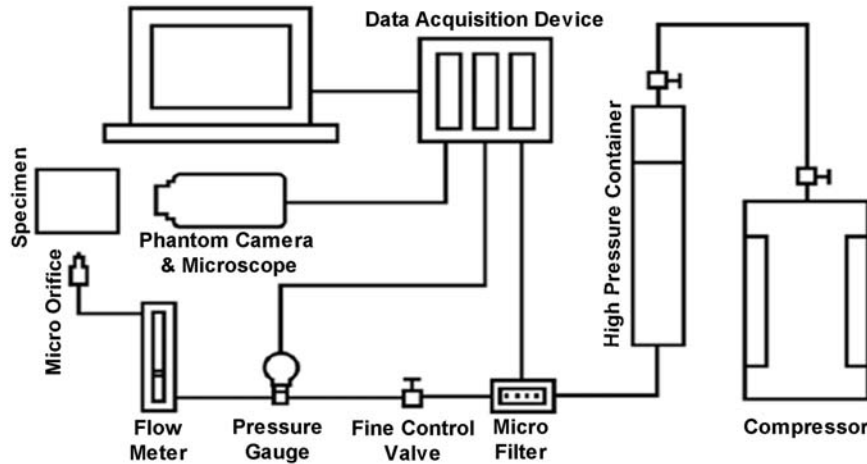


Figure 1 Schematic representation of the hydrodynamic bubble cavitation set-up. The liquid ($1\times$ PBS) flows from the high-pressure container to the downstream tubing containing a micro filter, a fine control valve tuning flow, pressure gauge and a flow meter documenting both pressure and flow. Emerging bubbles expand at the end of the micro orifice containing a microprobe, and are targeted to the desired spot on the specimen. A Phantom camera and microscope are connected to a data acquisition device and are used to document the experiments

of 80–100°C, causing coagulation necrosis of the targeted areas as well as the surrounding tissues. This may lead to various degrees of nerve and vessel damage and damage to normal tissues.^{21,22} Usage of the HIFU method overcome these limitations and results in highly focused target destruction. Similarly, the histotripsy method minimizes side effects through usage of focused intense bursts ultrasound, leading to precise tissue destruction by cavitation rather than thermal mechanisms.

Effects of ultrasonic cavitation on benign prostate hyperplasia (BPH) were studied extensively.^{23–25} BPH is a common health problem caused by overproliferation of the prostate tissue leading to the narrowing of the urethra lumen in middle and older aged males. Cases that do not respond to drug treatment require open or transurethral surgical resection or laser vaporization. Ultrasound-based treatments provided promising results for non-invasive treatments of BPH. HIFU studies were used for the thermal coagulation treatment of the aberrant tissue. On the other hand, cavitation generated by histotripsy methods were successfully used to achieve therapeutic level prostate tissue ablation in canine models of the disease.

Here, we used hydrodynamic bubble cavitation as an alternative method of cavitation generation for biomedical purposes. We have previously shown that hydrodynamic cavitation could kill leukemia cells in suspension culture and erode calcium oxalate kidney stones.^{26,27} In this work, we tested the efficacy of hydrodynamic cavitation in killing prostate cells in culture and its potential to ablate BPH tissues. The molecular mechanisms of the destructive effects of hydrodynamic cavitation were also analyzed in detail. In the light of our results with cells in culture and surgically excised human tissue samples, here we demonstrate that cavitation produced by hydrodynamic methods might be used as a promising experimental tool in the treatment of BPH.

Materials and methods

Experimental set-up for hydrodynamic bubble cavitation generation

Our experimental set-up was as previously described.²⁶ A schematic presentation of the experimental set-up is shown in Figure 1. Briefly, a pressure driven flow through a 0.5 cm long polyether ether ketone (PEEK) probe with an inner diameter of 147 μm , was used as a flow restrictive orifice leading to low local pressures and generation of hydrodynamic bubble cavitation. Pressure values between 50 and 150 psi were applied to the inlet of the orifice, while the exit pressure was set to atmospheric pressure. The probes were cleaned by sonication and all equipments and solutions were sterilized in 70% ethanol and autoclaved prior to usage. Phosphate buffered saline (PBS) was used as the physiological solution circulated in the system.

Characterization and measurement of cavitation

During the experiments, it was observed that cavitation inception at a pressure of ~ 500 kPa. By increasing the pressure beyond this point more distinct bubbles were recorded. The bubble cloud and bubble emergence at the exit of the orifice was captured by a double frame Phantom V320 high speed camera along with a light microscope unit and image processing Phantom software. Based on the captured images by the high speed camera, the sizes of bubbles targeted to the samples varied from 60 to 300 μm (Supplementary Figure 1).

Although it is not possible to measure cavitation directly, cavitation intensity might be expressed through calculation of the “cavitation number”. The cavitation number, σ , is a dimensionless number used for quantifying similar cavitating conditions and for representing the intensity of cavitation. It can be quantified by the difference between the local static pressure head and vapor pressure head divided by the velocity head. It is defined as:

$$\sigma = \frac{p_{\infty} - p_v}{(1/2)\rho v_{th}^2}$$

A reduction in cavitation number will increase the intensity and the extent of the cavitation. The channel geometry also affects the formation of cavitation.

Here, the maximum pressure value was imposed by the maximum available pressure for the present experimental set-up measured as 9600 kPa and the the flow rate was measured as 1.9 mL/s. Under the conditions of the maximum applied pressure, the corresponding cavitation number was deduced as $\sigma \sim 0.014$ (Supplementary Figure 1). This value lies within the range of the existing micro scale cavitation studies.

Cell line, cell culture

PC-3 and DU-145 human prostate carcinoma cells were cultured in Dulbecco's modified Eagle's medium (DMEM; Biological Industries) supplemented with 10% (v/v) fetal bovine serum (FBS; PAN, P30-3302), 2 mmol/L L-glutamine and antibiotics (100 μ g penicillin/100 U streptomycin; Biological Industries, 03-031-1B) in a 5% CO₂-humidified incubator at 37°C.

Cavitation pressure and exposure time kinetics experiments

Prostate cells PC-3 and DU-145 were trypsinized, washed and resuspended in PBS in 75 cm² flasks at a density of 10⁶ cells/mL. Hydrodynamic cavitation was applied for durations of 1–5 min, and using inlet pressures between 50 and 150 psi. Following exposure, the cells were collected, centrifuged at 300 \times g for 5 min, plated in culture medium and incubated for an additional 24 h as indicated.

Trypan blue exclusion tests

Following the application of cavitation, the cells were centrifuged at 300 \times g for 5 min, carefully washed and resuspended in fresh medium. Cell viability was determined with the trypan blue (Sigma, #T8154) exclusion assay. Cells treated with 8 μ mol/L Staurosporine (Sigma, #S5921), 10 μ mol/L Cisplatin (Sigma, #P4394) or 50 μ mol/L Etoposide (Sigma, # E1383) were used as controls.

DNA ladder analysis

Genomic DNA was isolated as described previously.²⁸ Briefly, following cavitation application, cells were lysed in the lysis buffer (1% NP-40, 20 mmol/L EDTA and 50 mmol/L Tris-Cl, pH: 7.5). After centrifugation (1600 \times g for 5 min at 4°C), 1% sodium dodecyl sulfate (SDS) and 0.5 μ g/ μ L RNase A were added to the supernatants and incubated at 56°C for 2 h. Consecutive proteinase K (Promega, # V3021) treatment (5 μ g/ μ L) was performed at 37°C for 2 h. Then DNA was precipitated using 0.5 volume 10 mol/L ammonium acetate and 2.5 volume 100% ethanol. Samples were washed in 70% ethanol and separated in 2% agarose gels.

Antibodies and immunoblotting

Primary anti-cleaved caspase 3 (#9661; 1/1000 dilution), anti-cleaved caspase 8 (#9496; 1/1000 dilution) and anti-poly ADP ribose polymerase (anti-PARP; #9542, 1/5000 dilution) antibodies were purchased from Cell Signaling. Anti-LC3 (#L7543; 1/2000 dilution) and anti- β -actin (#A5441, 1/4000 dilution) antibodies were purchased from Sigma-Aldrich. Anti-p62 (#610832, 1/1000 dilution) antibody was purchased from BD Transduction Laboratories. Secondary anti-mouse (#115035003, 1/20.000 dilution) or anti-rabbit (#111035144, 1/20.000 dilution) were purchased from Jackson Immunoresearch Laboratories.

For immunoblotting, cells were lysed in 50–150 μ L of immunoprecipitation assay buffer (25 mmol/L Tris, 125 mmol/L NaCl, 1% Nonidet P-40, 0.1% SDS, 0.5% sodium deoxycholate, 0.004% sodium azide, pH 8.0) supplemented with complete protease inhibitor cocktail (Roche, 04-693-131-001) and 1 mmol/L phenylmethylsulfonyl fluoride (Sigma-Aldrich, P7626). Proteins were separated using 10% or 15% SDS-polyacrylamide gels (SDS-PAGE) and then transferred onto nitrocellulose membranes (Millipore, IPVH00010). The membranes were blocked in 5% non-fat milk in PBST (3.2 mmol/L Na₂HPO₄, 0.5 mmol/L KH₂PO₄, 1.3 mmol/L KCl, 135 mmol/L NaCl, 0.05% Tween 20, pH 7.4) for 1 h and then incubated with a 3% bovine serum albumin containing PBST solution with primary antibodies. Following washes in PBST, the membranes were incubated with horseradish peroxidase coupled secondary antibodies and washed. Bands were displayed by chemiluminescence followed by X-ray film exposure (Fujifilm).

Cell cycle analysis

The cells were cultured after cavitation (150 psi, 5 min), trypsinized at indicated time points, washed in PBS and fixed in ice cold 70% ethanol. Then, the ethanol was discarded and the cells were resuspended in PBS. Following treatment with 100 μ g/mL RNase A (Sigma, # R6513) for 30 min at 37°C, propidium iodide (PI) (Invitrogen, # P3566) was added at a final concentration of 40 μ g/mL and the cells were incubated for an additional 30 min. The cell cycle was analyzed using a FACSCanto flow cytometer (Becton Dickinson) and the Cell Quest (Becton Dickinson) software.

Cavitation tests and analysis of human benign prostatic hyperplasia (BPH) tissues

All experiments were approved by the Maltepe, Sabanci and Yeditepe Universities' Ethics Committees and patient consent forms were collected. Human benign prostate tissue samples were obtained from Maltepe University Hospital. The cavitation tests were performed no later than 2–3 h after the operation. The tissue samples were drop stained in the Shandon Tissue Marking dye (Thermo Scientific), and exposed to bubble cavitation (\sim 9600 kPa) for 15 min. Cavitation exposed areas were devoid of the dye covering the surface of the tissue. As a control for the shear effect, PBS was applied with a similar flow rate but under conditions not leading to the generation of cavitation bubble. At the end of the experiments, tissues were fixed in 10% buffered formaldehyde solution. Prostate tissues were then embedded into paraffin, and 4 μ m

thick tissue sections were obtained from the paraffin blocks. Following deparaffinization in xylene and rehydration through a graded ethanol series (3×5 min.), the sections were stained with hematoxylin and eosin (H&E) dyes according to standard protocols. Stained BPH tissue sections were examined by a pathologist using fluorescence microscopy (Leica).

Statistical analyses

The Student's *t*-test was used for statistical analyses. Values of $P < 0.05$ were considered as significant.

Results

Hydrodynamic cavitation application led to a reduction in prostate cell numbers

To identify the effect of hydrodynamic cavitation on prostate cells, PC-3 and DU-145 cell lines were exposed to bubble cavitation created using a set of increasing initial pressure values (50, 100 and 150 psi). Cells were harvested immediately after exposure or they were cultured for up to 24 h following cavitation. Cell numbers and cell death ratios were determined at these time points. As shown in Figure 2(a), a significant decrease in cell numbers was observed following the application of cavitation in PC-3 prostate cells. This decrease was proportional to the pressure applied. Yet, at any time point checked, the percentage of dying cells did not exceed 10% (Figure 2(b)). Moreover, cell death ratios did not increase following incubation of cells for up to 24 h. Therefore, cavitation killed PC-3 prostate cells during the exposure period, and no

delayed effects on cell survival were observed following the recovery phase of cells in incubation. Similar results were observed with the DU-145 prostate cell line (Figure 2(c) and (d)).

Effect of hydrodynamic cavitation exposure time on cell numbers and cell death

Next, we checked whether the cavitation exposure time affected cell numbers and cell death. The inlet pressure was set to 150 psi and the cells were exposed to cavitation for 1, 2, 3 or 5 min. Cell numbers and cell death ratios were determined immediately after cavitation exposure (0 h) or following an incubation time of 24 h. As shown in Figure 3(a), an exposure time-dependent decrease in PC-3 cell numbers was observed. Again, the percentage of dead cells right after cavitation exposure (0 h) or following 24 h of incubation was not higher than 12% of total PC-3 cell numbers (Figure 3(b)). Similar results were obtained with DU-145 cells (Figure 3(c) and (d)).

All of these results showed that cavitation caused a dramatic decrease in the number of prostate cells exposed. The damage caused by cavitation was immediate, destroying a significant proportion of cells and leaving only a small percentage of detectable damaged cells.

Exploration of the mechanism responsible for cavitation-induced cell death

Although we could obtain only a small fraction of the cells damaged after cavitation experiments, we wondered whether hydrodynamic cavitation could lead to the activation of

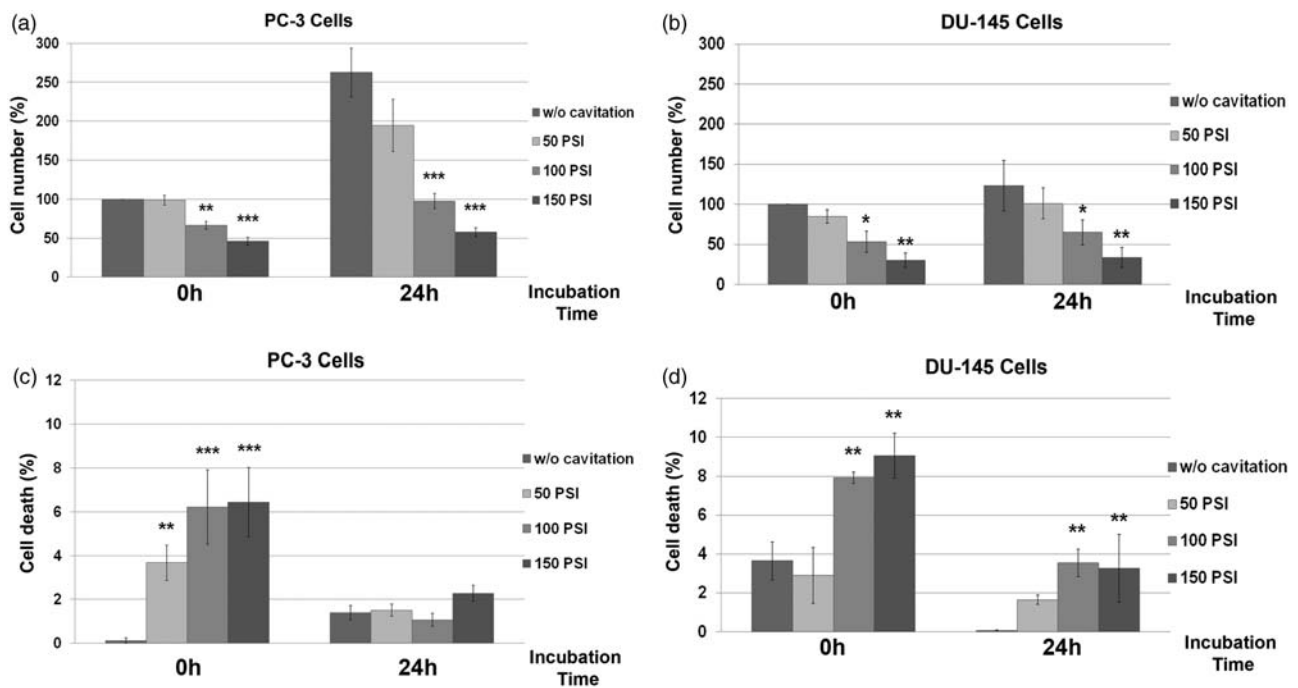


Figure 2 Effect of hydrodynamic cavitation on prostate cancer cell number and survival. Prostate cancer cells PC-3 and DU-145 were exposed for 5 min to hydrodynamic cavitation produced by 50, 100 and 150 psi inlet pressures. Cells were analyzed immediately after cavitation (0 h) or following 24 h incubation. w/o cavitation are the controls not exposed to cavitation. PC-3 and DU-145 cell numbers (a and c, $n = 3$) and death (b and c, trypan blue exclusion assay, $n = 3$) were documented relative to the controls. Data are shown as mean \pm standard deviation (Student's *t*-test, * $P < 0.05$, ** $P < 0.01$, *** $P < 0.001$)

programmed cell death pathways in prostate cells. In fact, in vitro studies by others showed that ultrasonic cavitation killed cells through the activation of apoptosis, a classical form of programmed cell death.²⁹ The morphological characteristics of apoptosis include the rounding and detachment of cells, chromatin condensation, nuclear fragmentation and apoptotic body formation. At a molecular level, the activation of cell death-related hydrolases called caspases is defined as one of the hallmarks of apoptosis. Caspase activation results in the cleavage of substrates relevant to cell survival including PARP and DNA itself.

The cell death results in Figures 2 and 3 were obtained using the trypan blue exclusion technique. Trypan blue is a vital dye only penetrating cells when the cell membrane has lost its integrity. Therefore, we first wanted to confirm our observations using another technique. We treated PC-3 cells with Hoechst (coloring all nuclei in blue) and PI (entering only dying cells and coloring nuclei in red) fluorescent dyes and analyzed them under a fluorescent microscope (Figure 4(a)). PC-3 cells treated under control conditions or exposed to 150 psi cavitation were compared. In-line with the trypan blue data, only a small percentage of PI positive cells were detected following cavitation exposure. Nuclei of the majority of cells did not show prominent death-related changes, i.e. there was no visible chromatin condensation, nuclear fragmentation or apoptotic body formation. Yet, nuclear changes were observed in a few PI positive cells that could be detected. Therefore, cells surviving cavitation trauma seemed to have a healthy morphology.

Apoptotic changes at a molecular level including caspase activation occur before the morphological changes ensue. Therefore, we analyzed the activation of caspase-3 and caspase-8 in PC-3 cells exposed to cavitation produced by 50,

100 or 150 psi inlet pressure. We used cells exposed to established apoptosis inducer chemicals, staurosporine or cisplatin as controls. As shown in Figure 4(b), although active caspase bands appeared in staurosporine or cisplatin-treated cells, with increasing pressure, and hence the cavitation forces, did not result in the appearance of active caspase-3 or caspase-8 bands in PC-3 cells. Lack of caspase activation was observed in cells analyzed immediately after cavitation application (0 h) or following 24 h incubation. In-line with these results, there was no cleavage of caspase-3/-6 substrate PARP following 0 h or 24 h after cavitation exposure (Figure 4(c)). Similarly, PARP cleavage was not observed in DU-145 cells in response to cavitation (Figure 4(d)). Next, the effect of exposure time was investigated. In PC-3 cells, application of 150 psi of pressure did not lead to caspase-3 or caspase-8 activation (Figure 4(e)) or to PARP cleavage (Figure 4(f)) following 1, 2, 3 or 5 min exposure to cavitation. PARP cleavage following cavitation application was not observed in DU-145 cells either (Figure 4(g)). Therefore, cavitation did not activate apoptosis-related caspase activation in PC-3 and DU-145 prostate cells.

DNA fragmentation and damage following hydrodynamic cavitation exposure

During apoptosis, cleavage of caspase-3 target inhibitor of caspase activated DNase (ICAD) allows the caspase activated DNase (CAD) enzyme to enter the nucleus and fragment the DNA at internucleosomal sites, giving rise to a typical ladder appearance. Therefore, we checked for DNA laddering in cells exposed to cavitation. In control cells treated with the apoptosis activator etoposide, we could observe formation of a clear DNA ladder in agarose gels (Figure 5(a)). Yet, no laddering could be observed in the DNA of cells exposed to hydrodynamic cavitation. Interestingly, there was no evidence

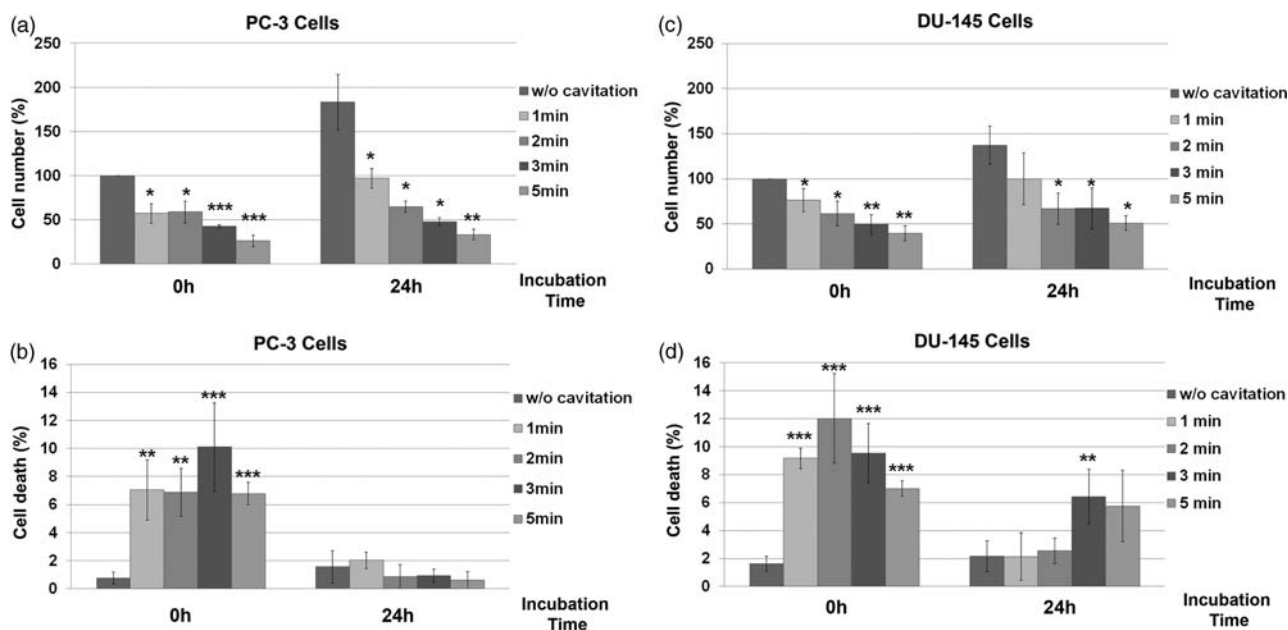


Figure 3 Effect of cavitation exposure time on prostate cancer cell number and survival. PC-3 and DU-145 were exposed for 1, 2, 3 or 5 min. to hydrodynamic cavitation produced by 150 psi inlet pressure. Cells were analyzed immediately after cavitation (0 h) or following 24 h incubation. w/o cavitation are the controls not exposed to cavitation. PC-3 and DU-145 cell numbers (a and c, $n = 4$) and death (b and c, trypan blue exclusion assay, $n = 3$) were documented relative to controls. Data are shown as mean \pm standard deviation (Student's *t*-test, * $P < 0.05$, ** $P < 0.01$, *** $P < 0.001$)

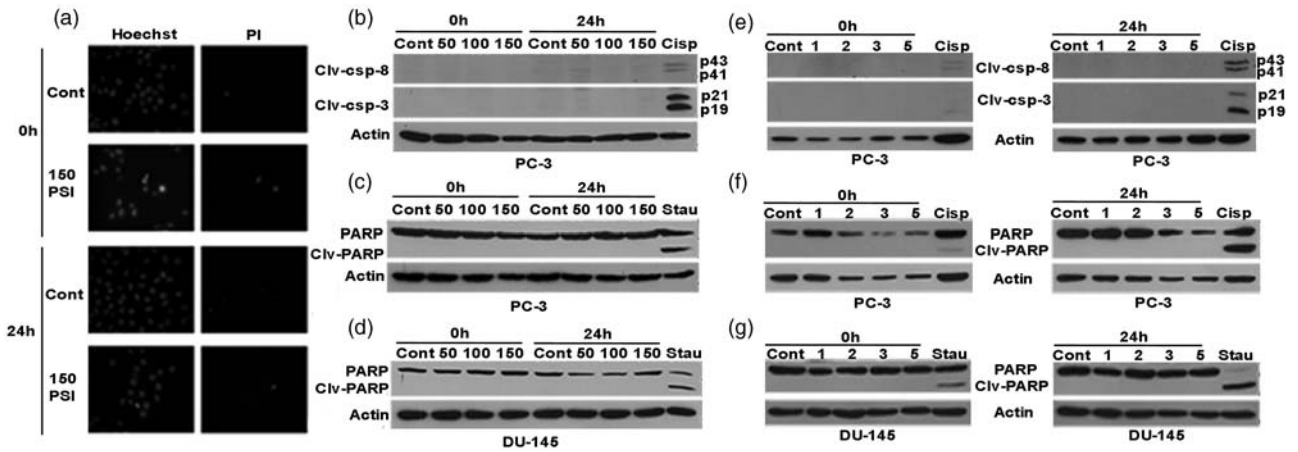


Figure 4 Apoptosis markers in cavitation-exposed prostate cells. a, Documentation of dead cells in cavitation exposed populations. Hoechst and PI staining pictures of control, non-treated PC-3 cells or cells exposed to cavitation (150 psi). b–g, Pressure- (b–d, 50, 100, 150 psi) and time- (e–g, 1, 2, 3, 5 min) dependent analysis of apoptosis molecular markers in cavitation-exposed cells. Cisp (cisplatin, 10 $\mu\text{mol/L}$) and Stau (staurosporine, 8 $\mu\text{mol/L}$) were used as positive controls. Analysis of caspase-8 and caspase-3 (b and e) and PARP cleavage (c, d, f, g) in PC-3 (b, c, e, f) and DU-145 (d and g) prostate cells. Clv-csp, cleaved caspase. Clv-PARP, cleaved PARP

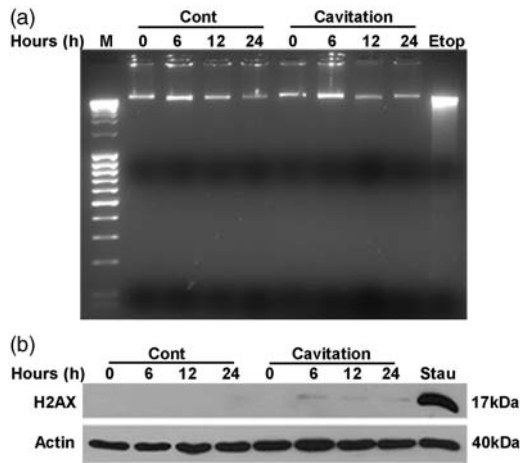


Figure 5 DNA fragmentation and DNA damage following hydrodynamic cavitation exposure. PC-3 cells were exposed to 150 psi, 5 min cavitation and cultured for 0–24 h. Cont samples are from control unexposed cells. A, DNA laddering test. The fragmentation on genomic DNA was visualized on 2% agarose gel. Etop, etoposide (50 $\mu\text{mol/L}$) used as a positive control. B, Immunoblots showing the level of H2AX phosphorylation (a DNA damage marker) in cells exposed to hydrodynamic cavitation. Stau, Staurosporine used as a positive control

of larger DNA fragments either, suggesting that cavitation did not mechanically break the DNA of intact cells into detectable pieces.

During apoptosis, DNA fragmentation leads to the appearance of a hypodiploid sub-G1 fraction of cells. Therefore, cell cycle analyses were performed in PC-3 cells exposed to hydrodynamic cavitation. We observed no significant sub-G1 fraction accumulation in exposed cells compared to controls (Supplementary Figure 2). Furthermore, cavitation-treated cells did not show any cell cycle change or cell cycle arrest at the time points analyzed.

A few breaks resulting from cavitation-induced DNA damage could still be present in the genomes of exposed cells and cellular mechanisms could be activated to repair

this damage. A widely used technique to detect the abundance of double strand DNA breaks consists of the analysis of a phosphorylated form of the Histone 2AX protein (phospho-H2AX) in cell extracts. H2AX is known to be phosphorylated on serine 139 by damage sensing kinases and this event serves to mark DNA damage sites and facilitates access for the repair machinery. Therefore, we checked the level of H2AX phosphorylation in the extracts of cells exposed to hydrodynamic cavitation. As shown in Figure 5(b), although extracts from staurosporine-treated control treated cells showed prominent H2AX phosphorylation in immunoblots, and hence had double strand DNA breaks, cells exposed to cavitation possessed no significant amount of phospho-H2AX (Figure 5(b)).

Altogether, the results presented above showed that cavitation did not lead to DNA fragmentation or damage in the prostate cells exposed.

Autophagy in cavitation exposed prostate cells

Autophagy is a stress response allowing cells to survive growth factor and nutrient starvation or insults including hypoxia, drugs and toxins. Autophagy is also a major recycling mechanism for long-lived proteins, protein aggregates and damaged organelles.³⁰ In some scenarios, programmed cell death was shown to depend on the activation of autophagy and autophagy proteins.^{31,32} Therefore, we checked whether autophagy was activated in cells exposed to cavitation. For the detection of autophagy, we used two classical autophagy markers: we analyzed the degradation of the autophagy receptor p62, and checked the lipidation of the autophagy protein LC3B in immunoblots.^{33,34} Autophagy-related lipidation of LC3 converts free LC3-I (18 kDa) into a faster migrating, autophagosome-associated LC3-II form (16 kDa). As shown in Figure 6(a), p62 protein degradation was not observed in PC-3 cells exposed to cavitation produced by 50, 100 or 150 psi pressures. Moreover, although control staurosporine-treated cells activated autophagy, no clear LC3-II shift was observed in cells exposed to 50 or 100 psi cavitation, whereas 150 psi cavitation led to a mild LC3-II shift (Figure 6(b)). Similar

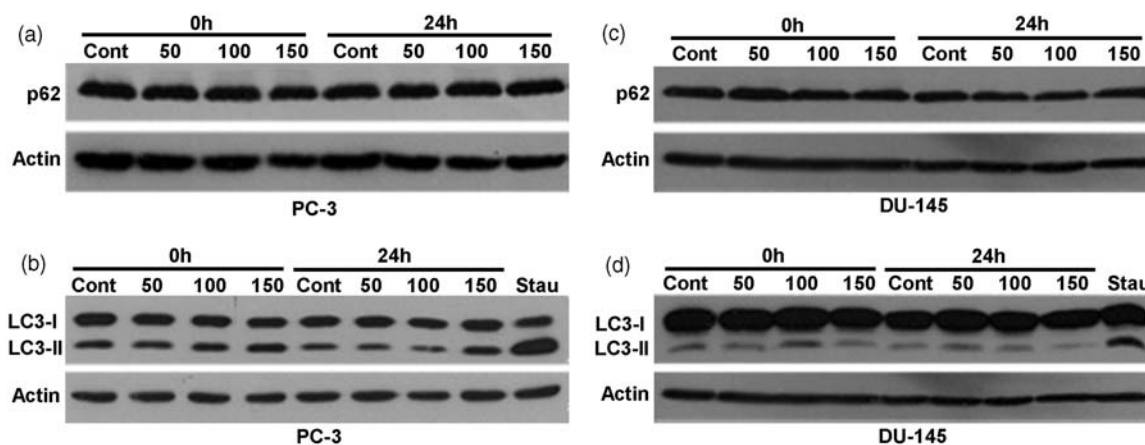


Figure 6 Autophagy in cavitation exposed prostate cells. PC-3 (a and b) or DU-145 (c and d) cells were exposed 5 min to 50, 100 or 150 psi, 5 min cavitation. a and c, Degradation of the autophagy target p62 protein was analyzed by immunoblotting. b and d, Lipidation and autophagic vesicle recruitment of the MAP1-LC3 (LC3) protein analyzed by immunoblotting. Conversion of the free LC3-I form into LC3-II correlates with autophagy activation. Cont, control unexposed samples. Stau, staurosporine- (8 $\mu\text{mol/L}$) treated positive controls

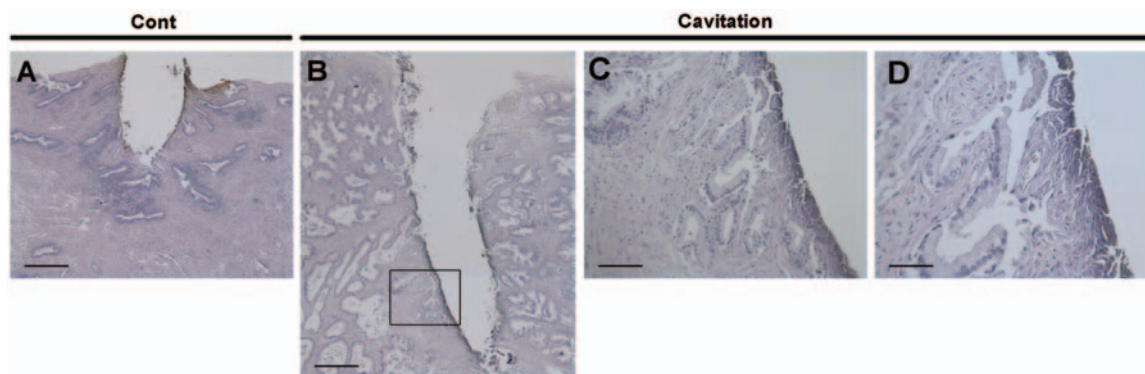


Figure 7 Effect of hydrodynamic cavitation on fresh human BPH tissue specimens. Tissues were exposed for 15 min to hydrodynamic cavitation produced by 1450 psi pressure (b–d) or a PBS jet at same flow rate but without cavitation (a, Cont, control). Histopathological analysis using H&E staining was shown (a, b, 5 \times ; c, 20 \times ; D, 40 \times magnification). Square in b indicates magnified region shown in c and d. Similar results were obtained in four independent experiments. Scale bar: 400 μm (a and b); 100 μm (c) and 50 μm (d)

experiments were performed in DU-145 cells, confirming that cavitation did not prominently activate autophagy (Figure 6(c) and (d)).

Ablation of human BPH tissue specimens through the application of hydrodynamic cavitation

We have showed that hydrodynamic cavitation application led to pressure and application time-dependent massive death of two different prostate cells in culture, namely PC-3 and DU-145 cells. Encouraged by results obtained with prostate cells, we wanted to test in our set-up the destructive effects of cavitation on surgically removed human BPH tissues (average size 10 mm \times 10 mm \times 5–10 mm). Hydrodynamic cavitation with an inlet pressure 1450 psi (approximately 100 bar) was focally applied for 15 min onto freshly obtained BPH tissue specimens. As control, we used a larger gauge micro orifice probe allowing similar flow rates but not leading to cavitating bubble formation. The effects of cavitation on exposed tissues were assessed by histopathological analysis of the specimen following H&E staining. As seen in Figure 7, cavitation led to clear and prominent damage to the exposed

BPH tissue specimen compared to non-cavitating controls. We also see penetrating effect of cavitation into the depth of tissue. Although the shear forces of the flushed liquid could contribute to some of the observed effects on tissues, application of the liquid with cavitating bubbles led to the formation of deeper and more focused areas of damage.

Discussion

In this study, we analyzed the effects of cavitation on prostate cells and tissues. We showed that cavitation led to a decrease in prostate cell numbers in a pressure- and time-dependent manner. Yet, the fraction of detectable trypan blue- or PI-positive dead cells did not reflect the magnitude of the decrease in cells. Culture of cells for 24 h after cavitation exposure led to a further decrease in the numbers of dead cells. Under these conditions, cavitation did not lead to the activation of apoptosis, shown here by the analysis of nuclear changes, caspase activation, PARP cleavage, sub-G1 fraction cells and DNA laddering. Prominent activation of autophagy by cavitation was not observed either. All of these results strongly indicated that cavitation damaged cells instantly,

leading to the pulverization of cells immediately after exposure, leaving no intact damaged cells to be analyzed. Interestingly, the remaining cells did indeed recover and showed neither DNA damage nor cell cycle changes or arrest. Hence, survivors in cell culture were probably those cells that were undamaged, or cells that were eventually repaired.

Ultrasonic treatment of cells or tissues was reported to cause cell death with various mechanisms. While low intensity ultrasound cavitation caused a transient disruption of membranes cells in tissues,^{29,35,36} high frequency ultrasound led to irreversible cellular damage either resulting in instant cell lysis or in the induction of programmed cell death (mainly apoptosis) *in vitro*.³⁷ Moreover, *in vivo* application of high frequency ultrasound resulted in tissue damage through necrosis or apoptosis.^{23,24} Mitochondria-dependent apoptotic signaling pathway was shown to be activated by ultrasound in some studies.³⁸ Autophagy was also activated as a stress response following ultrasonic treatment of cells and chemical inhibition of autophagy enhanced cell death.^{39,40} Under our experimental conditions, we did not observe robust apoptosis activation or autophagic responses. The observed discrepancy might stem from differences in the characteristics of the cavitation produced by different techniques. The amount of generated cavitation bubbles, their sizes and energy released following bubble collapse might not be the same in hydrodynamic versus ultrasonic cavitation. Moreover, the behavior of the bubble cloud produced by these two techniques might also be different. Off note, in our experimental set-up, cavitation probe was directly in contact with cells in suspension allowing a homogenous and close contact with the cavitation cloud. Therefore, the dominant effect of hydrodynamic cavitation generated in our set-up seems to be irreversible cell membrane damage rather than a more delayed and indirect apoptotic response.

Hydrodynamic cavitation-based methods offer several advantages. In fact, usage of hydrodynamic cavitation for biotechnology-related goals including microbial cell (*Escherichia coli* and yeast) disruption,^{41,42} sterilization of waste waters^{43,44} and fluids⁴⁵ biodiesel production²⁵ and nano-particle generation⁴⁶ was suggested. The technique is cost-effective and it is also energy-efficient. It creates modulable yet powerful destructive forces. In addition to its physical effects, the implosion of the bubbles may lead to the local generation of reactive oxygen species in liquid media, enhancing the destructive effects of hydrodynamic cavitation in biological contexts. Moreover, heat-production by hydrodynamic cavitation is localized; therefore, heat-related side effects in the surrounding tissues are not expected in the case of hydrodynamic cavitation.

We acknowledge that compared to ultrasonic methods, hydrodynamic cavitation has limitations. The system requires a flow tube in order to create negative pressure and the treatment can only be performed in tissues where the tip of the device can be positioned. This limitation is not faced by other cavitation technologies based on focused ultrasound, including histotripsy. Therefore, *in vivo* applications and clinical use of hydrodynamic cavitation might only be possible through the integration of the cavitation tube system into an endoscopy device. It is also critical that precise manipulation

of the endoscopic cavitation probe would be achieved in body cavities such as urethra in the case of BPH treatment, in such a way to allow application of the cavitation in a user-defined, localized and targeted manner. To overcome these limitations, we are currently developing a computer assisted and robotically manipulated version of an endoscope-integrated hydrodynamic cavitation device.

In-line with studies on ultrasonic cavitation of prostate cells and tissues,^{6–11} results obtained in this study showed that hydrodynamic cavitation treatment should be considered as a promising experimental treatment strategy for the treatment of BPH. Further studies including *in vivo* animal studies followed by clinical studies are needed to reveal the full potential of this technique.

Author contributions: All of the authors participated in the design, interpretation of the studies and analysis of the data and review of the manuscript. ZI and OO conducted most of the experiments. OYP, MS, ED and AK contributed to the hydrodynamic cavitation design and settings. SE supplied BPH tissue, IDE helped in histochemical analysis. DG had overall responsibility for the work and the manuscript.

ACKNOWLEDGMENTS

This work was supported by Sabancı University Internal Grant for Research Program under Grant IACF09-00642 and the Scientific and Technological Research Council of Turkey (TUBITAK) 1001 Grant (Project No: 111M621). D.G. is a recipient of EMBO Strategical Development and Installation Grant (EMBO-SDIG) and D.G. and A.K. are recipients of a Turkish Academy of Sciences (TUBA) GEBIP Award. The authors have no financial conflict of interests.

REFERENCES

1. Rooney JA. Shear as a mechanism for sonically induced biological effects. *J Acoust Soc Am* 1972;52:1718–24
2. Rooney JA. Hydrodynamic shearing of biological cells. *J Biol Phys* 1973;2:26–40
3. Povey MJWMT (ed.). *Ultrasound in Food Processing*, 1st edn. London: Blackie Academic & Professional, 1998:283
4. Madersbacher S, Pedevilla M, Vingers L, Susani M, Marberger M. Effect of high-intensity focused ultrasound on human prostate cancer *in vivo*. *Cancer Res* 1995;55:3346–51
5. Uchida T, Muramoto M, Kyunou H, Iwamura M, Egawa S, Koshiba K. Clinical outcome of high-intensity focused ultrasound for treating benign prostatic hyperplasia: preliminary report. *Urology* 1998;52:66–71
6. Xu Z, Ludomirsky A, Eun LY, Hall TL, Tran BC, Fowlkes JB, Cain CA. Controlled ultrasound tissue erosion. *IEEE Trans Ultrasonics Ferroelect Freq Control* 2004;51:726–36
7. Lake AM, Hall TL, Kieran K, Fowlkes JB, Cain CA, Roberts WW. Histotripsy: minimally invasive technology for prostatic tissue ablation in an *in vivo* canine model. *Urology* 2008;72:682–86
8. Hall TL, Hempel CR, Wojno K, Xu Z, Cain CA, Roberts WW. Histotripsy of the prostate: dose effects in a chronic canine model. *Urology* 2009;74:932–37
9. Hempel CR, Hall TL, Cain CA, Fowlkes JB, Xu Z, Roberts WW. Histotripsy fractionation of prostate tissue: local effects and systemic response in a canine model. *J Urol* 2011;185:1484–89
10. Styn N, Hall TL, Fowlkes JB, Cain CA, Roberts WW. Histotripsy homogenization of the prostate: thresholds for cavitation damage of periprostatic structures. *J Endourol/Endourol Soc* 2011;25:1531–35

11. Schade GR, Keller J, Ives K, Cheng X, Rosol TJ, Keller E, Roberts WW. Histotripsy focal ablation of implanted prostate tumor in an ACE-1 canine cancer model. *J Urol* 2012;188:1957–64
12. Wu F, Wang ZB, Cao YD, Chen WZ, Bai J, Zou JZ, Zhu H. A randomised clinical trial of high-intensity focused ultrasound ablation for the treatment of patients with localised breast cancer. *Br J Cancer* 2003;89:2227–33
13. Wu F, Wang ZB, Cao YD, Chen WZ, Zou JZ, Bai J, Zhu H, Li KQ, Jin CB, Xie FL, Su HB, Gao GW. Changes in biologic characteristics of breast cancer treated with high-intensity focused ultrasound. *Ultrasound Med Biol* 2003;29:1487–92
14. Wu F, Chen WZ, Bai J, Zou JZ, Wang ZL, Zhu H, Wang ZB. Pathological changes in human malignant carcinoma treated with high-intensity focused ultrasound. *Ultrasound Med Biol* 2001;27:1099–106
15. Miller DL, Song J. Tumor growth reduction and DNA transfer by cavitation-enhanced high-intensity focused ultrasound in vivo. *Ultrasound Med Biol* 2003;29:887–93
16. Wu F, Wang ZB, Zhu H, Chen WZ, Zou JZ, Bai J, Li KQ, Jin CB, Xie FL, Su HB. Extracorporeal high intensity focused ultrasound treatment for patients with breast cancer. *Breast Cancer Res Treat* 2005;92:51–60
17. Chapelon JY, Margonari J, Vernier F, Gorry F, Ecochard R, Gelet A. In vivo effects of high-intensity ultrasound on prostatic adenocarcinoma Dunning R3327. *Cancer Res* 1992;52:6353–57
18. Sibille A, Prat F, Chapelon JY, abou el Fadil F, Henry L, Theilliere Y, Ponchon T, Cathignol D. Characterization of extracorporeal ablation of normal and tumor-bearing liver tissue by high intensity focused ultrasound. *Ultrasound Med Biol* 1993;19:803–13
19. Duryea AP, Maxwell AD, Roberts WW, Xu Z, Hall TL, Cain CA. In vitro comminution of model renal calculi using histotripsy. *IEEE Trans Ultrasonics Ferroelectr Freq Control* 2011;58:971–80
20. Duryea AP, Roberts WW, Cain CA, Hall TL. Controlled cavitation to augment SWL stone comminution: mechanistic insights in vitro. *IEEE Trans Ultrasonics Ferroelectr Freq Control* 2013;60:301–9
21. Wu F, Wang ZB, Cao YD, Xu ZL, Zhou Q, Zhu H, Chen WZ. Heat fixation of cancer cells ablated with high-intensity-focused ultrasound in patients with breast cancer. *Am J Surg* 2006;192:179–84
22. Blana A, Rogenhofer S, Ganzer R, Wild PJ, Wieland WF, Walter B. Morbidity associated with repeated transrectal high-intensity focused ultrasound treatment of localized prostate cancer. *World J Urol* 2006;24:585–90
23. Balasundaram B, Harrison ST. Study of physical and biological factors involved in the disruption of *E. coli* by hydrodynamic cavitation. *Biotechnol Prog* 2006;22:907–13
24. Balasundaram B, Harrison ST. Disruption of Brewers' yeast by hydrodynamic cavitation: process variables and their influence on selective release. *Biotechnol Bioeng* 2006;94:303–11
25. Sunstrom NA, Premkumar LS, Premkumar A, Ewart G, Cox GB, Gage PW. Ion channels formed by NB, an influenza B virus protein. *J Membr Biol* 1996;150:127–32
26. Kosar A, Sesen M, Oral O, Itah Z, Gozuacik D. Bubbly cavitating flow generation and investigation of its erosional nature for biomedical applications. *IEEE Trans Bio-med Eng* 2011;58:1337–46
27. Perk OY, Sesen M, Gozuacik D, Kosar A. Kidney stone erosion by micro scale hydrodynamic cavitation and consequent kidney stone treatment. *Ann Biomed Eng* 2012;40:1895–902
28. Hermann T, Meier T, Gotte M, Heumann H. The 'helix clamp' in HIV-1 reverse transcriptase: a new nucleic acid binding motif common in nucleic acid polymerases. *Nucleic Acids Res* 1994;22:4625–33
29. Ashush H, Rozenszajn LA, Blass M, Barda-Saad M, Azimov D, Radnay J, Zipori D, Rosenschein U. Apoptosis induction of human myeloid leukemic cells by ultrasound exposure. *Cancer Res* 2000;60:1014–20
30. Gozuacik D, Kimchi A. Autophagy as a cell death and tumor suppressor mechanism. *Oncogene* 2004;23:2891–906
31. Gozuacik D, Bialik S, Raveh T, Mitou G, Shohat G, Sabanay H, Mizushima N, Yoshimori T, Kimchi A. DAP-kinase is a mediator of endoplasmic reticulum stress-induced caspase activation and autophagic cell death. *Cell Death Differ* 2008;15:1875–86
32. Gozuacik D, Kimchi A. Autophagy and cell death. *Curr Top Dev Biol* 2007;78:217–45
33. Guzman HR, Nguyen DX, Khan S, Prausnitz MR. Ultrasound-mediated disruption of cell membranes. II. Heterogeneous effects on cells. *J Acoust Soc Am* 2001;110:597–606
34. Guzman HR, Nguyen DX, Khan S, Prausnitz MR. Ultrasound-mediated disruption of cell membranes. I. Quantification of molecular uptake and cell viability. *Journal Acoust Soc Am* 2001;110:588–96
35. Feril LB Jr, Kondo T, Cui ZG, Tabuchi Y, Zhao QL, Ando H, Misaki T, Yoshikawa H, Umemura S. Apoptosis induced by the sonomechanical effects of low intensity pulsed ultrasound in a human leukemia cell line. *Cancer Lett* 2005;221:145–52
36. Lagneaux L, de Meulenaer EC, Delforge A, Dejeneffe M, Massy M, Moerman C, Hannecart B, Canivet Y, Lepeltier MF, Bron D. Ultrasonic low-energy treatment: a novel approach to induce apoptosis in human leukemic cells. *Exp Hematol* 2002;30:1293–301
37. Vykhodtseva N, McDannold N, Martin H, Bronson RT, Hynynen K. Apoptosis in ultrasound-produced threshold lesions in the rabbit brain. *Ultrasound Med Biol* 2001;27:111–17
38. Firestein F, Shemesh-Darvish L, Elimelech R, Radnay J, Rosenschein U. Induction of apoptosis by ultrasound application in human malignant lymphoid cells: role of mitochondria-caspase pathway activation. *Ann N Y Acad Sci* 2003;1010:163–66
39. Wang P, Xu C. Low-intensity ultrasound-induced cellular destruction and autophagy of nasopharyngeal carcinoma cells. *Exp Ther Med* 2011;2:849–52
40. Wang X, Liu Q, Wang Z, Wang P, Zhao P, Zhao X, Yang L, Li Y. Role of autophagy in sonodynamic therapy-induced cytotoxicity in S180 cells. *Ultrasound Med Biol* 2010;36:1933–46
41. Franke M, Braeutigam P, Wu ZL, Ren Y, Ondruschka B. Enhancement of chloroform degradation by the combination of hydrodynamic and acoustic cavitation. *Ultrasonics Sonochem* 2011;18:888–94
42. Wang X, Wang J, Guo P, Guo W, Wang C. Degradation of rhodamine B in aqueous solution by using swirling jet-induced cavitation combined with H₂O₂. *J Hazard Mater* 2009;169:486–91
43. Milly PJ, Toledo RT, Chen J, Kazem B. Hydrodynamic cavitation to improve bulk fluid to surface mass transfer in a nonimmersed ultraviolet system for minimal processing of opaque and transparent fluid foods. *J Food Sci* 2007;72:M407–13
44. Milly PJ, Toledo RT, Harrison MA, Armstead D. Inactivation of food spoilage microorganisms by hydrodynamic cavitation to achieve pasteurization and sterilization of fluid foods. *J Food Sci* 2007;72:M414–22
45. Ji J, Wang J, Li Y, Yu Y, Xu Z. Preparation of biodiesel with the help of ultrasonic and hydrodynamic cavitation. *Ultrasonics* 2006;44(Suppl 1): e411–4
46. Christman CL, Carmichael AJ, Mossoba MM, Riesz P. Evidence for free radicals produced in aqueous solutions by diagnostic ultrasound. *Ultrasonics* 1987;25:31–4

(Received March 26, 2013, Accepted July 22, 2013)